INTERNATIONAL JOURNAL OF MARITIME TECHNOLOGY
IJMT Vol.18/Spring & Summer 2023 (15-24)
Available online at: www. ijmt.ir

Calculation of Hydrodynamics Resistance Coefficient of Diver by CFD Method at Free Surface Condition

Nima Khanmoradi[1*], Mohammad Moonesun[2], Sara Jafari Horestani[3]

[1] *Department of Mechanical Engineering, Sharif University of Technology, Tehran, Iran; nimakhanmoradi.edu@gmail.com*
[2]*Department of Civil & Architectural Engineering, Shahrood University, Shahrood, Iran; m.moonesun@gmail.com*
[3]*Department of Physical Education and Sport Sciences, Kharazmi University, Tehran, Iran; sara1995jafari@gmail.com*

ARTICLE INFO

Article History:
Received: 08 Apr 2023
Accepted: 05 Jun 2023

Keywords:
human body
diver resistance
swimmer resistance
CFD
resistance coefficient
free surface simulation

ABSTRACT

The aim of the present study is calculation of the resistance and resistance coefficient of a diver on the water surface and near surface. The results of this article are useful for designing different types of water scooters. This study uses a computational fluid dynamics methodology by considering the effects of free surface. SST K-ω turbulent model is implemented in the Star-CCM+ application and is applied to the flow around a three-dimensional bare hull of an adult human. Three common swimming positions are considered: a ventral position with the arms extended at the front, a ventral position with the arms placed alongside the trunk and a ventral position with one arm extended at the front and another arm placed alongside the trunk. The flow velocities between 0.5 and 2.25m/s with increasing step of 0.25m/s are considered in the simulations which are typical speed of swimmers. According to the resistance coefficient vs Froude number diagrams, submerged diving with two hands alongside the trunk is produces lower resistance. Also, resistance in near surface swimming is lower than surface swimming in lowest speeds. But in higher speeds, that changes and resistance in surface swimming is lower than the other. The results of this research can be used for designing all types of marine propulsion vehicles, water scooter, and all swimming thrusters.

1. Introduction

Resistance and resistance coefficient in different velocities during submerged swimming (single phase) for three usual positions of swimming is calculated by CFD method [1]. This article says that how different positions of diving affect on resistance and resistance coefficient based on cross-section area and wetted area. Also, there is similar study for a diver with diving equipment by Khanmoradi that shows how diving equipment contribute to increasing the resistance of diver during the swimming [2].

The passive resistance of male swimmer during underwater movement in a streamlined position has been measured experimentally [3,4]. Their results suggest that a three-dimensional CFD analysis of a swimmer could provide useful information about resistance. Swimming performance is determined by the combined effect of propulsion, drag and technical skill [5]. Passive drag, it can be considered as a relevant predictor of gliding performance during the underwater phases of the starts and turns, which are important components of the overall swimming event [6]. Lyttle found that reduction of the hydrodynamic resistance during the glide can lead to turning times reduction [7]. The most common method used to study the passive drag acting in human swimming is by towing subjects at various velocities, body positions and depths using electro-mechanical motors or weights and pulley systems [8,9,10,11]. However, other methods are being used, like the Inverse Dynamics [12] and computational fluid dynamics [3,13,14,15]. The CFD method is a numerical modelling technique that can be applied for

extracting the hydrodynamic phenomena, and is used as an acceptable method to the experimental research regarding the determination of a swimmer's passive resistance. Also, the effect of depth is checked with a three-dimensional method [16]. The resistance coefficient for other underwater vehicles is calculated. The mathematical models of the drag coefficients of the hull shape genealogy with different shape parameters and Reynolds numbers were established by fitting the data obtained from CFD calculation. The accuracy of the established drag coefficient models was verified by the tank tests [17].

Both experimental and numerical analyses on the bare hull Resistance coefficient of a submarine at snorkel condition and surface condition is done by Moonesun and co-workers. The Comparison of the results of submarine bare hull resistance by CFD and experimental methods shows some differences in low Froude numbers but a good adjustment in the usual range of Froude of submarines [18]. Also, there is a study on minimizing the resistance of the bare hull form of submarines [19]. The comparison of simulation and experimental results shows that the results of Flow Vision software are reliable in CFD modeling.

Effect of slenderness ratio and aft fins on the hydrodynamic forces for an underwater body in oblique flows is investigated [20]. The body in this article is torpedo shaped with elliptical nose, tapered tail and cylindrical middle body. Pressure measurements and flow visualization were done and compared with CFD flow field predictions.

According to the history, all the existing researches are devoted to providing the resistance of the swimmer's body in streamline form. Most of these have been analyzed in the swimming pool with wall boundary condition. Now, there is a gap in existing researches regarding the body resistance of a diver or swimmer with a non-streamline body shape in the sea. There are many marine propulsion vehicles and different types of water scooters that are used to make the movement of swimmers and divers easier and faster.

These vehicles can be used for both recreational and military swimming. Many of them are used only for the movement of ordinary people without diving equipment, and many of them are used to facilitate the movement of divers in military missions (Figure 1).

Figure 1. Different Types of Underwater Scooters [21,22]

To have an ideal design of these vehicles, the present study will be very useful. Therefore, by considering the available types of thrusters, the different states of a swimmer's body have been created in CAD (Computer-Aided Design) and resistance and resistance coefficient is extracted.

2. Three-Dimensional Model Specification

At the first step, a bare body model of an adult real human was modeled in CAD. The basic 3D model that is used for the analysis include head, chest, waist, and hip circumferences, is shown in Figure 2. Also, all lengths and dimensions are specified in Figure 3.

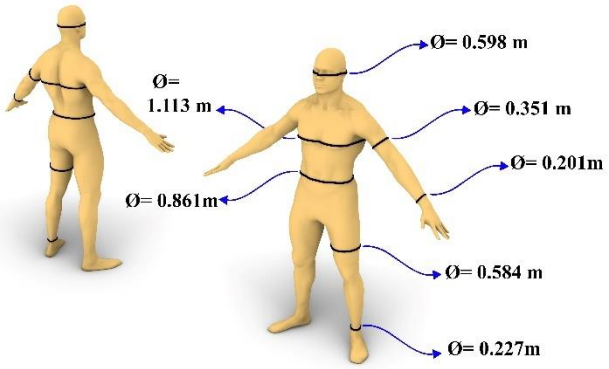

Figure 2. Main Geometry head, chest, waist, and hip circumferences

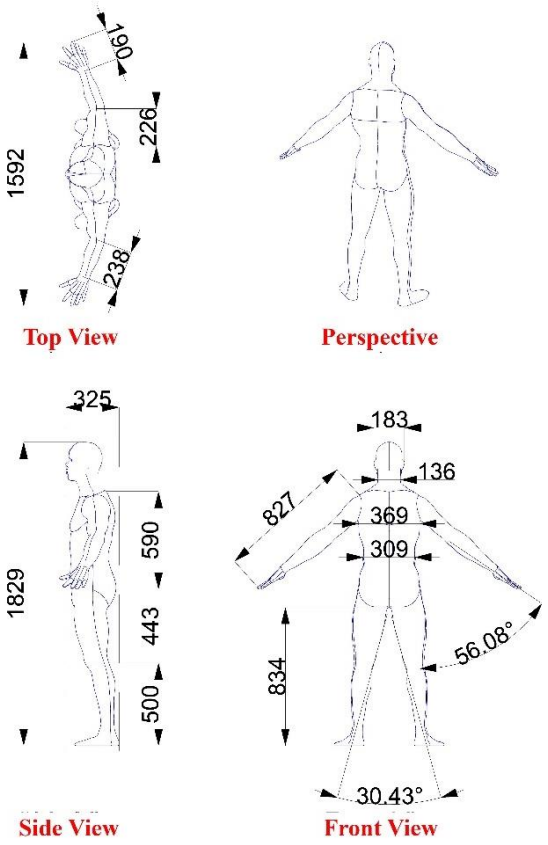

Figure 3. Main Geometry Dimension and Specifications

After that, the different positions are extracted from the main geometry according to the different models of thrusters (**Error! Reference source not found.**).

The geometry number 1 is the body shape of a normal swimmer in a ventral position with the arms extended at the front. It is compatible with two-handed thrusters. geometry number 2 that swimmer is in a ventral position with the arms placed alongside the trunk. Finally, geometry number 3 is a combination of two geometries 1 and 2, which shows a ventral position with one arm extended at the front and another arm placed alongside the trunk. It is suitable for designing of single handle thrusters. The cross-section areas for geometries 1 to 3 are 0.108, 0.142 and 0.125 m^2 respectively. These areas are calculated by projecting all cross sections on a surface at the front and considering the maximum area. Also, the wetted areas are 2.111, 2.073 and 2.092 m^2.

Mentioned values for cross-section Area and wetted area was for near surface swimming. For surface mode, the draught of the trunk in still water is considered. Therefore, the cross-section areas for geometries 1 to 3 are 0.083, 0.115 and 0.099 m^2 and the wetted areas are 1.577, 1.557 and 1.567 m^2respectively.

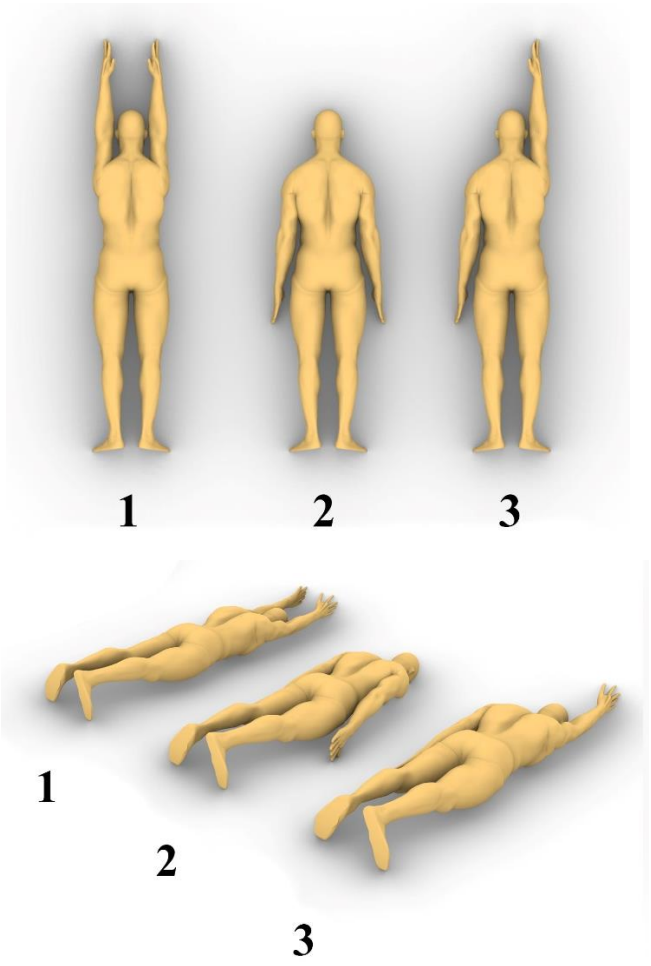

Figure 4. Figure 4. All geometries for analyzing

3. CFD Simulation

All the simulations are analyzed with the body in a horizontal position with an attack angle of 0°. The attack angle is defined as the angle between a horizontal line and a line drawn from the vertex to the ankle bone.

The boundary conditions of the computational fluid dynamics model are designed to represent the geometry and flow conditions of a part of a lane in the open water. “Velocity Inlet”, “Pressure Outlet” and “Symmetry Plan” are chosen for boundary condition for domain. “Wall’ condition is chosen for swimmer’s body as well.

Domain dimensions and boundary condition are shown in Figures 5 to 7.

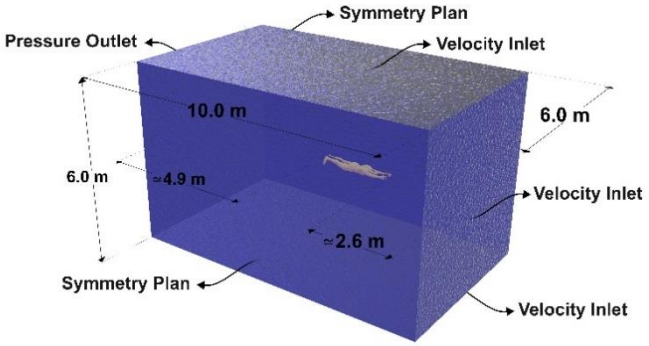

Figure 5. Domain and Boundary Condition Prespective View

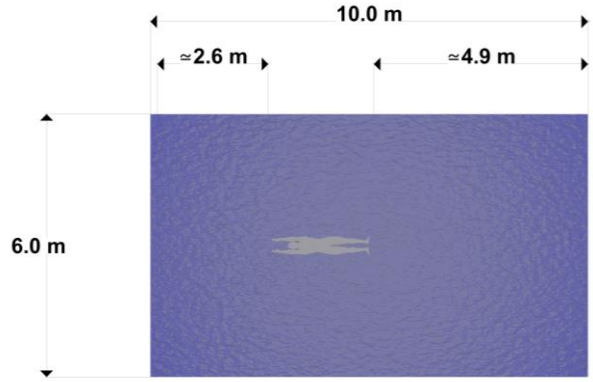

Figure 6. Domain and Boundary Condition Top View

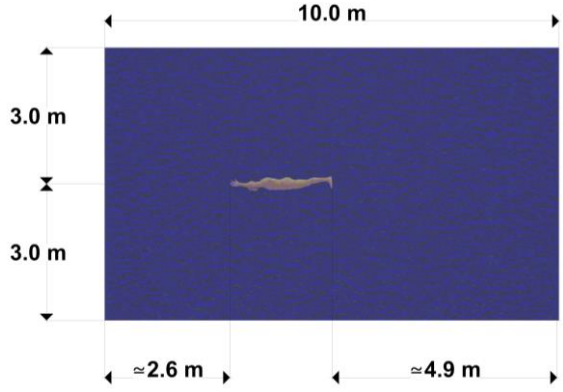

Figure 7. Figure 6. Domain and Boundary Condition Side View

Also, the swimmer model middle line is placed equidistant from the top and bottom boundaries.

A half of domain is used for symmetrical geometries to reduce cell numbers and time of each solving.

The type of implemented mesh is trimmed cell with prism layers. Significant efforts are conducted to ensure that the model would provide accurate results namely by decreasing the grid node separation in areas of high velocity and pressure gradients. Mesh independency is also checked that results are shown in Figure 8 diagram.

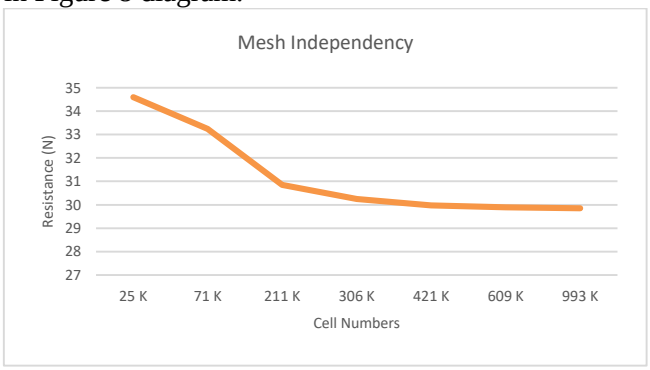

Figure 8. Mesh Independency Diagram

After checking mesh independency, about 421,000 cell numbers are used for the symmetrical analysis. The implemented networking mesh on Geometry 1 is shown in Figure 9.

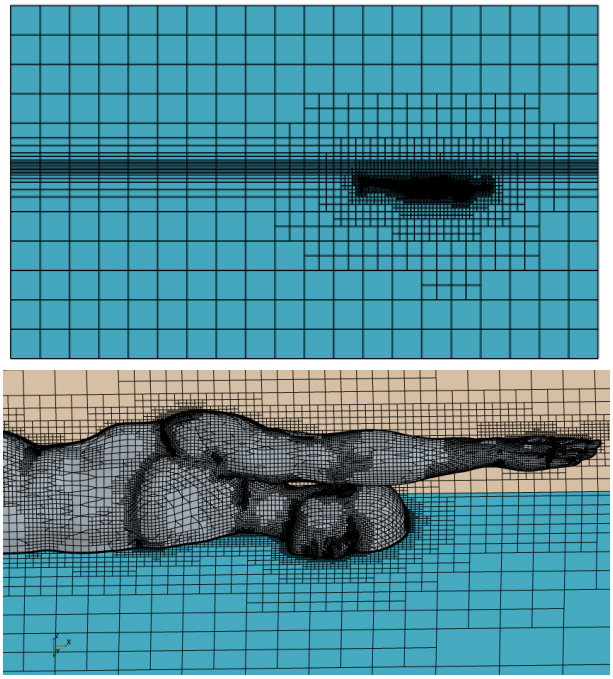

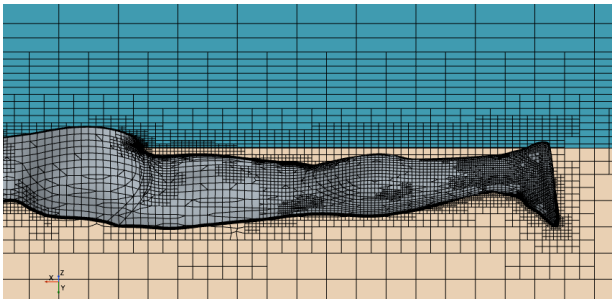

Figure 9. Trimmed Cell Mesh Implemented on Geometry No.1.

Implemented prism layer has 0.005 m thickness include 8 layers with 1.2 grow rate stretching. Also, first node distance is about 0.0005m (Figure 10).

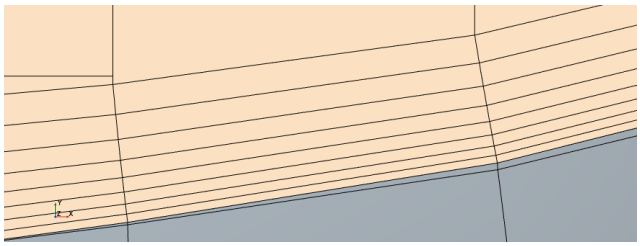

Figure 10. Implemented Cell Mesh in Prism Layer Region

Based on it, Y+ contour in shown in figure 11 and related plot is shown also in figure 12.

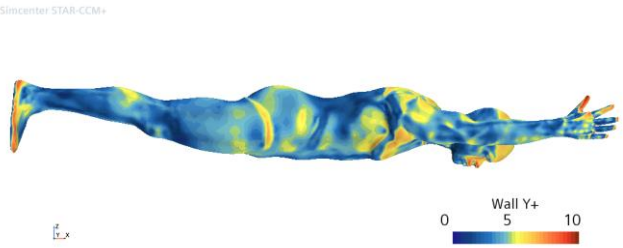

Figure 11. Y+ Contour on the body of diver

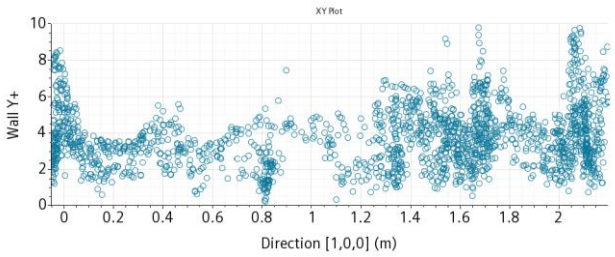

Figure 12. Y+ plot in all length of diver

The main parameters of CFD simulation are shown in Table 1. In this table, solving parameters of our CFD simulations are shown in two parts of "Initial Conditions" and "Physics".

Table 1. Main Parmeters of CFD Simulations

Initial Conditions	***Roughness***	0
	Water Temperature	28 °C
	Water Density	997.561 kg/m^3
	Air Density	1.18415 kg/m^3
Physics	Three Dimensional	
	Implicit Unsteady	
	K-ω Turbulence	
	Multiphase	
	Multiphase Interaction	
	Reynolds-Averaged Navier-Stokes	
	Segregated Flow	
	SST (Menter) K-ω	
	Transition Boundary Distance	
	Turbulence Suppression	
	Turbulent	
	Volume of Fluid (VOF) Waves	
	Gravity	

Based on the value of speed and the size of smallest mesh cell, the value of 0.001 sec is considered for time-step.

Segregated solver with standard SST K-ω turbulence model is used, because this turbulence model is shown to be accurate with measured values in another research [23].

Resistance and resistance coefficient are calculated for velocities ranging from 1.50 to 2.25 m/s in increments of 0.25 m/s that are equal with Froude number from 0.106 to 0.525. Flow velocities are chosen to be within the range of typical underwater swimming.

All analyzes are done in two different depths. One on them is swimming on the surface of water and the other one is swimming 0.25m below water surface. The initial position of swimmer in each depth of swimming is shown in Figure 13.

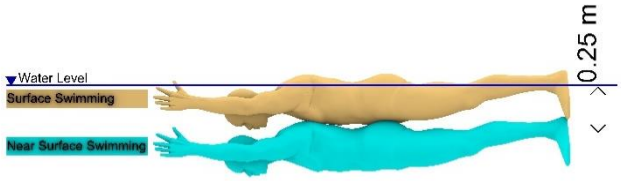

Figure 13. Swimmer positions at Near surface and Surface Swimming

4. Validation for CFD Simulation

Validation with existing articles is necessary at the first step of numerical simulation. So, geometry number 1 in figure 3 is used for comparison with Maria's article [16]. Table 2 is a general comparison between the geometry used in Maria's article and the geometry in this study.

Table 2. A comparison between the geometries used in this study and Maria's paper

		Maria L. [16]	***Geometry No. 1***
Lengths	Height	1.90 m	1.83 m
	Finger to Toe	2.40 m	2.40 m
Circumferences	Head	0.58 m	0.59 m
	Chest	1.02 m	1.11 m
	Waist	0.87 m	0.86 m
	Hip	0.93 m	0.89 m

Our validation results are shown in Table 3. Maximum error for validation based on resistance coefficient is about 8.85 percent that is acceptable.

Based on this, we can continue our simulation for all the geometries.

Table 3. Validation Results

Depth (m)	*Speed (m/s)*	*Maria L. Results [15]*	*This Study Results*	*Error (%)*
0	1.5	0.625	0.685	5.280
	2.0	0.6	0.602	0.311
0.25	1.5	0.756	0.739	2.214
	2.0	0.662	0.721	8.85

5. Results and Discussions

Two phases modeling for geometry No. 1 for both depths of swimming are shown in Figure 14. These contours are for speed of 2.25 m/s. Also, velocity vectors around the body are shown in each situation.
Pressure contour around the body is shown in Figure as sample. These all are at speed of 2.25 m/s.
Also, Free surface modeling and wave pattern for geometry No. 1 for surface swimming is shown in Figure .

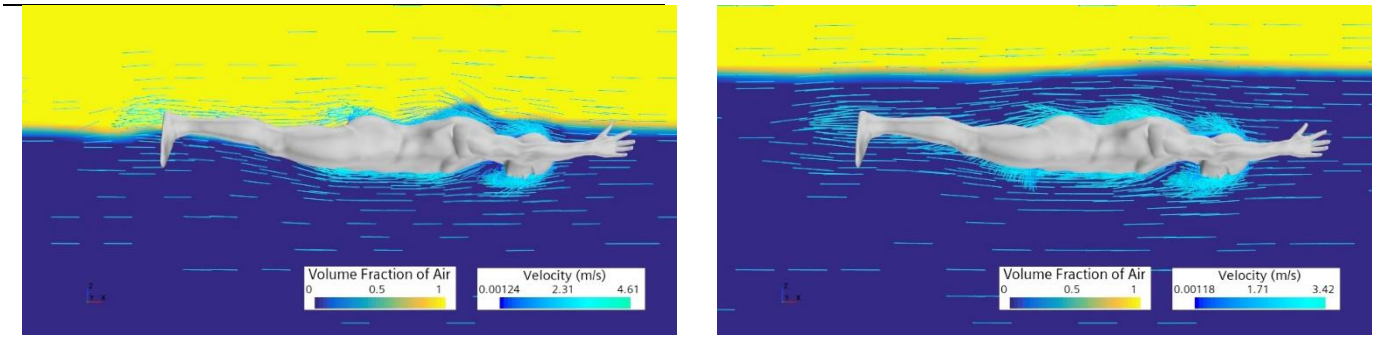

(a) Surface Swimming (b) Near Surface Swimming

Figure 14. Free Surface and Velocity Vectors Contour

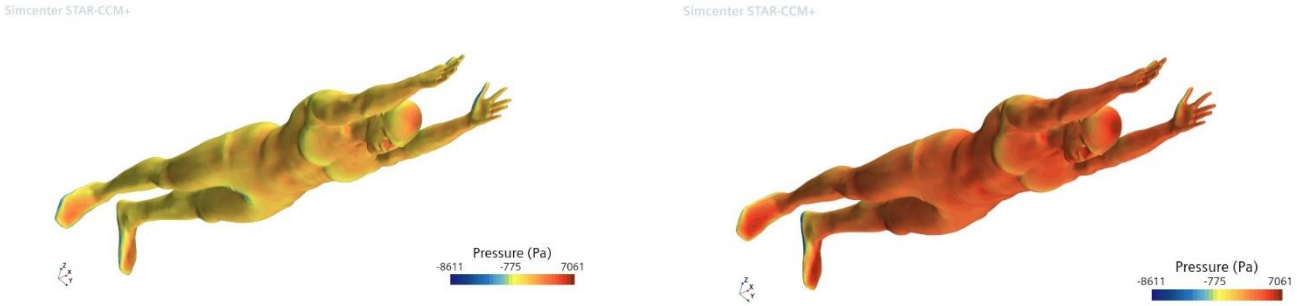

(a) Surface Swimming (b) Near Surface Swimming

Figure 15. Pressure Contour

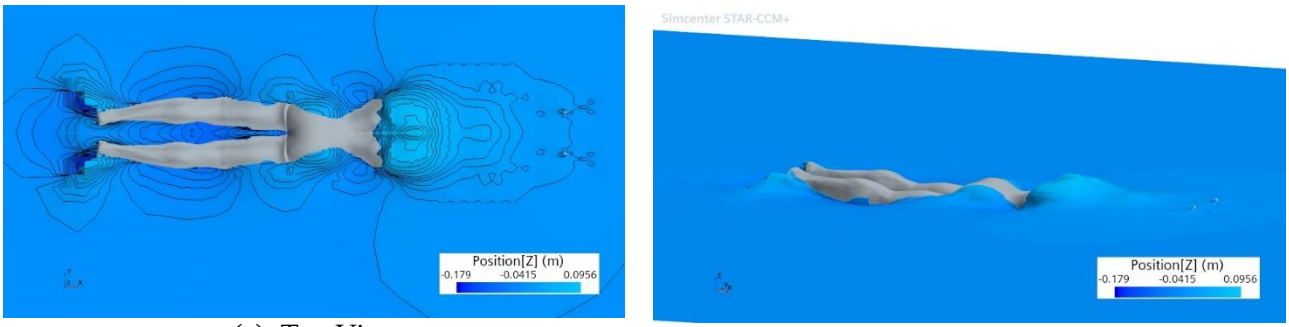

(a) Top View (b) Perspective View

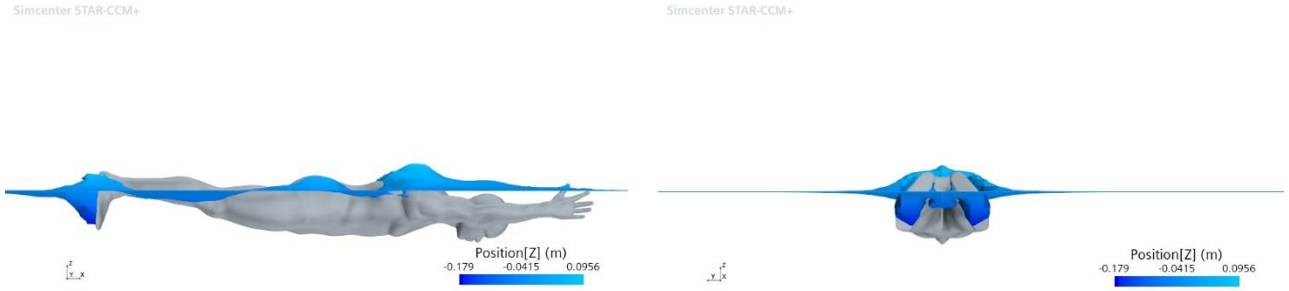

(c) Side View (d) Back View

Figure 16. Free Surface Visualizing Include Wave Pattern

Analyzing the resistance coefficient arising from three different positions in swimming through CFD method is the main aim of this study.

To analyze the relationship between velocity and resistance for different positions of swimming diagrams in Figure 17 are extracted.

For all the velocities, the resistance coefficient of the position with the arms extended at the front is higher than the resistance coefficient of the position with the arms along the trunk. Also, the geometry number 2 has resistance coefficient between geometries number 1 and 3 at most of speeds.

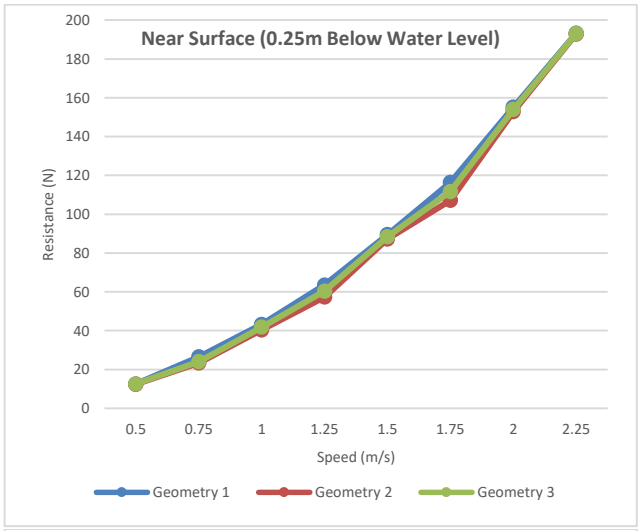

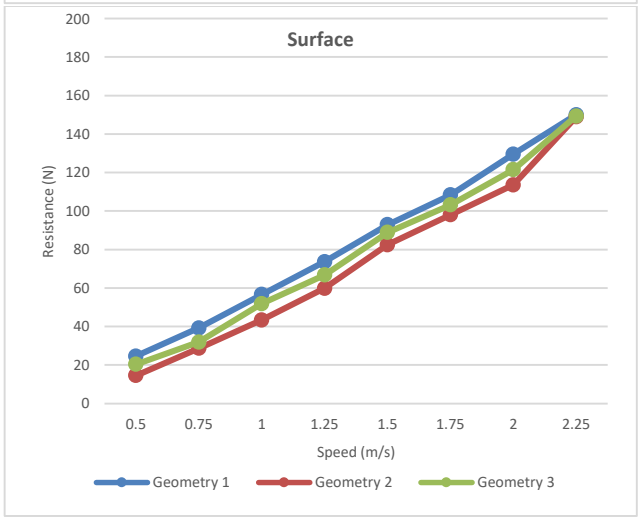

Figure 17. Resistance vs Speed Diagram for Different Swimming Positions.

The resistance coefficient for near surface swimming is various. It is from 0.9307 at 0.106 Froude number to 0.7092 at 0.479 Froude number, in the position with the arms extended at the front. It's Also from 0.6976 at 0.117 Froude number to 0.5382 at 0.525 Froude number, in the position with the arms along the trunk. Finally, it's from 0.8041 at 0.106 Froude number to 0.6122 at 0.479 Froude number, in position with one arm extended at the front and one arm alongside the trunk.

The resistance coefficient for surface swimming is various from 2.3710 at 0.106 Froude number to 0.7145 at 0.479 Froude number in the position with the arms extended at the front. It's also from 1.0171 at 0.117 Froude number to 0.5145 at 0.525 Froude number, in the position with the arms along the trunk. Finally, it is from 1.6495 at 0.106 Froude number to 0.5980 at 0.479 Froude number, in position with one arm extended at the front and one arm alongside the trunk.

Also, to analyze the relationship between Froude number and resistance coefficient for two different depths of swimming, diagrams in Figure 18 are extracted.

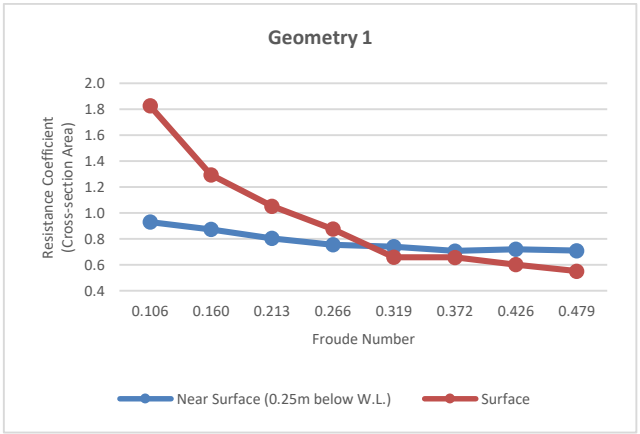

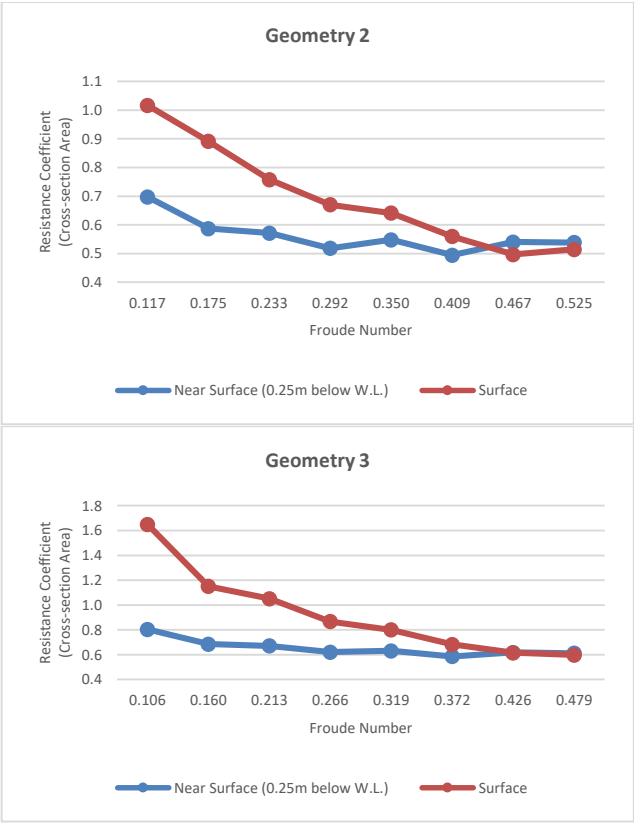

Figure 18. Resistance Coefficient vs Froude Number for Geometries No. 1 to 3.

6. Conclusion

The inverse relationship between the resistance coefficient and the velocity found in the current study seems to correspond to what happens in experimental situations with the human body totally submerged [24,10].

But about selection of the best shape of body during swimming on water surface and near surface, the position with the arms placed alongside the trunk has lowest resistance coefficient in comparison with the other body positions at most of speeds.

Also, for choosing the most suitable depth for swimming with any type of positions based on diagrams in Figure , for 1.75 m/s or lower velocities, swimming below water surface has lower resistance. However, for swimming at more than 2 m/s, being on water surface could be a better choice. As we have wave making resistance in both situations, this could be because of the differences between wetted areas [16].

Although limited to resistance, this study allows the evaluation of the effects of different body positions on performance Under the influence of free surface effects, being a first step toward the analysis of resistance. On the other hand, computational fluid dynamics methods have provided a way to estimate the relative contribution of each resistance component to the total resistance. Future studies could improve these computational fluid dynamics results by analyzing the effect of different equipment on swimming resistance during a surface or near surface swimming.

7. References

1- Khanmoradi, N., Moonesun, M., Jafari, H. S., (Under Revision). Calculation of Hydrodynamics Resistance Coefficient of Diver with Diving Equipment by CFD Method. Journal of Hydraulic and Water Engineering.

2- Khanmoradi, N., Moonesun, M., Jafari, H. S., (Under Revision). Calculation of Hydrodynamics Resistance Coefficient of Diver by CFD Method. Journal of Ships and Offshore Structures.

3- Bixler, B., Pease, D., & Fairhurst, F. (2007). The accuracy of computational fluid dynamics analysis of the passive drag of a male swimmer. Sports biomechanics, 6(1), 81-98.

4- Costa, L. C., Ribeiro, J., Marinho, D., Mantha, V., Vilas-Boas, J., Fernandes, R. J., ... & Machado, L. (2011). Comparing computational fluid dynamics and inverse dynamics methodologies to assess passive drag during swimming gliding. In ISBS-Conference Proceedings Archive.

5- Chatard, J. C., Lavoie, J. M., Bourgoin, B., & Lacour, J. R. (1990). The contribution of passive drag as a determinant of swimming performance. International journal of sports medicine, 11(05), 367-372.

6- D'Acquisto, M. A. (1988). Breaststroke economy, skill and performance study of breaststroke mechanics, using a computer based" Velocity. Video" system. Zentrum f. Wissenschaftsinformation, Körperkultur u. Sport.

7- Lyttle, A. D., Blanksby, B. A., Elliott, B. C., & Lloyd, D. G. (1998). The effect of depth and velocity on drag during the streamlined glide. Journal of Swimming Research, 13.

8- Counsilman, J. E. (1955). Forces in swimming two types of crawl stroke. Research Quarterly. American Association for Health, Physical Education and Recreation, 26(2), 127-139.

9- Kolmogorov, S. V., Rumyantseva, O. A., Gordon, B. J., & Cappaert, J. M. (1997). Hydrodynamic characteristics of competitive swimmers of different genders and performance levels. Journal of Applied Biomechanics, 13(1), 88-97.

10- Lyttle, A. D., Blanksby, B. A., Elliott, B. C., & Lloyd, D. G. (2000). Net forces during tethered simulation of underwater streamlined gliding and kicking techniques of the freestyle turn. Journal of Sports Sciences, 18(10), 801-807.

11- Toussaint, H. M., Roos, P. E., & Kolmogorov, S. (2004). The determination of drag in front crawl swimming. Journal of biomechanics, 37(11), 1655-1663.

12- Vilas-Boas, J. P., Costa, L., Fernandes, R. J., Ribeiro, J., Figueiredo, P., Marinho, D., ... & Machado, L. (2010). Determination of the drag coefficient during the first and second gliding positions of the breaststroke underwater stroke. Journal of applied biomechanics, 26(3), 324-331.
13- Zaidi, H., Taiar, R., Fohanno, S., & Polidori, G. (2008). Analysis of the effect of swimmer's head position on swimming performance using computational fluid dynamics. Journal of Biomechanics, 41(6), 1350-1358.
14- Marinho, D. A., Reis, V. M., Alves, F. B., Vilas-Boas, J. P., Machado, L., Silva, A. J., & Rouboa, A. I. (2009). Hydrodynamic drag during gliding in swimming. Journal of Applied Biomechanics, 25(3), 253-257.
15- Mollendorf, J. C., ALBERT C TERMIN, I. I., Oppenheim, E. R. I. C., & Pendergast, D. R. (2004). Effect of swim suit design on passive drag. Medicine & Science in Sports & Exercise, 36(6), 1029-1035.
16- Novais, M., Silva, A., Mantha, V., Ramos, R., Rouboa, A., Vilas-Boas, J., ... & Marinho, D. (2012). The effect of depth on drag during the streamlined glide: A three-dimensional CFD analysis. Journal of human kinetics, 33(2012), 55-62.
17- Liu, Y., Yu, Z., Zhang, L., Liu, T., Feng, D., & Zhang, J. (2021). A fine drag coefficient model for hull shape of underwater vehicles. Ocean Engineering, 236, 109361.
18- Moonesun, M., Ghasemzadeh, F., Korol, Y., Nikrasov, V., Yastreba, A., Ursolov, A., & Mahdian, A. (2016). Technical notes on the near surface experiments of submerged submarine. International Journal of Maritime Technology, 5, 41-54.
19- Moonesun, M., Korol, Y., & Dalayeli, H. (2015). CFD analysis on the bare hull form of submarines for minimizing the resistance. International Journal of Maritime Technology, 3, 1-16.
20- Praveen Perumpulissery Chandran, Krishnankutty Parameswaran & Panigrahi Prasanna Kumar (2018) Effect of slenderness ratio and aft fins on the hydrodynamic forces for an underwater body in oblique flows, Ships and Offshore Structures, 13:3, 256-264, DOI: 10.1080/17445302.2017.1357962.
21- dive-hurghada. (n. d.). PADI Diver Propulsion Vehicle Specialty (Scooter). https://www.dive-hurghada.com/prices/padi-scuba-diving-courses/padi-diver-propulsion-vehicle-specialty
22- finish-tackle. (n. d.). product. https://finish-tackle.com/product/magicjet-scooter/
23- Moreira, A., Rouboa, A., Silva, A. J., Sousa, L., Marinho, D., Alves, F., ... & Machado, L. (2006). Computational analysis of the turbulent flow around a cylinder. Portuguese Journal of Sport Sciences, 6(1), 105.
24- Jiskoot, J., & Clarys, J. P. (1975). Body resistance on and under the water surface. Swimming II, 2, 105-109.

Appendix A

In this appendix, exact numbers of resistance, resistance coefficient based on wetted area and resistance coefficient based on cross-section area are presented. These values are for geometries No.1 to No.3 in different velocities and Froude numbers.

Table A. 1: Amount of All Resistance and Resistance Coefficients

		Velocity (m/s)	*Froude Number*	*Resistance (N)*	*Resistance Coefficient (Cross-section Area)*	*Resistance Coefficient (wetted Area)*
Geometry 1	Near Surface (0.25m below W.L.)	0.5	0.106	12.52	0.9307	0.0475
		0.75	0.160	26.44	0.8736	0.0446
		1	0.213	43.24	0.8036	0.0410
		1.25	0.266	63.49	0.7552	0.0386
		1.5	0.319	89.5	0.7393	0.0378
		1.75	0.372	116.4	0.7064	0.0361
		2	0.426	155.1	0.7206	0.0368
		2.25	0.479	193.2	0.7092	0.0362
	Surface	0.5	0.106	24.58	1.8273	0.1249
		0.75	0.160	39.18	1.2945	0.0885
		1	0.213	56.64	1.0526	0.0720
		1.25	0.266	73.66	0.8761	0.0599
		1.5	0.319	92.9	0.6580	0.0525
		1.75	0.372	108.36	0.6576	0.0450
		2	0.426	129.54	0.6019	0.0412
		2.25	0.479	150	0.5507	0.0377
Geometry 2	Near Surface (0.25m below W.L.)	0.5	0.117	12.34	0.6976	0.0477
		0.75	0.175	23.36	0.5869	0.0402
		1	0.233	40.42	0.5712	0.0391
		1.25	0.292	57.32	0.5184	0.0355
		1.5	0.350	87.26	0.5481	0.0375
		1.75	0.409	107.1	0.4942	0.0338
		2	0.467	152.84	0.5400	0.0369
		2.25	0.525	192.8	0.5382	0.0368
	Surface	0.5	0.117	14.54	1.0171	0.0749
		0.75	0.175	28.66	0.8911	0.0656
		1	0.233	43.34	0.7580	0.0558
		1.25	0.292	59.88	0.6702	0.0493
		1.5	0.350	82.46	0.6409	0.0472
		1.75	0.409	98	0.5596	0.0412
		2	0.467	113.6	0.4967	0.0366
		2.25	0.525	148.94	0.5145	0.0379
Geometry 3	Near Surface (0.25m below W.L.)	0.5	0.106	12.52	0.8041	0.0480
		0.75	0.160	24.01	0.6853	0.0409
		1	0.213	41.82	0.6714	0.0401
		1.25	0.266	60.39	0.6205	0.0370
		1.5	0.319	88.38	0.6307	0.0376
		1.75	0.372	111.71	0.5856	0.0349
		2	0.426	153.99	0.6181	0.0369
		2.25	0.479	193.05	0.6122	0.0365
	Surface	0.5	0.106	20.34	1.6495	0.1040
		0.75	0.160	31.92	1.1505	0.0726
		1	0.213	51.89	1.0520	0.0664
		1.25	0.266	66.78	0.8665	0.0547
		1.5	0.319	88.86	0.8007	0.0505
		1.75	0.372	103.18	0.6831	0.0431
		2	0.426	121.52	0.6159	0.0389
		2.25	0.479	149.32	0.5980	0.0377